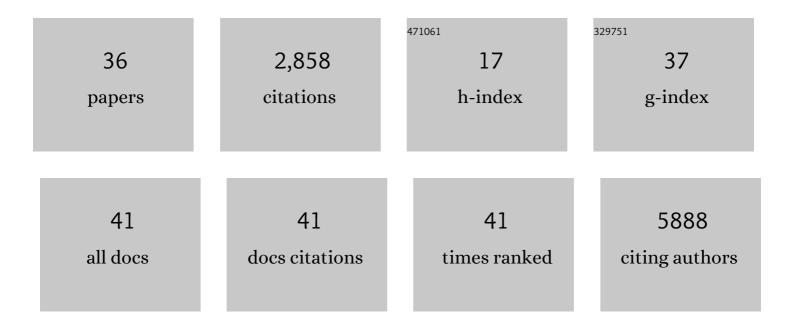
Alexis Vandenbon

List of Publications by Year in descending order

Source: https://exaly.com/author-pdf/8225045/publications.pdf Version: 2024-02-01



#	Article	IF	CITATIONS
1	Evaluation of critical data processing steps for reliable prediction of gene co-expression from large collections of RNA-seq data. PLoS ONE, 2022, 17, e0263344.	1.1	6
2	Cyclin J–CDK complexes limit innate immune responses by reducing proinflammatory changes in macrophage metabolism. Science Signaling, 2022, 15, eabm5011.	1.6	4
3	Enhancement of Regnase-1 expression with stem loop–targeting antisense oligonucleotides alleviates inflammatory diseases. Science Translational Medicine, 2022, 14, eabo2137.	5.8	8
4	Profibrotic function of pulmonary group 2 innate lymphoid cells is controlled by regnase-1. European Respiratory Journal, 2021, 57, 2000018.	3.1	30
5	Zinc Finger Protein St18 Protects against Septic Death by Inhibiting VEGF-A from Macrophages. Cell Reports, 2020, 32, 107906.	2.9	7
6	A clustering-independent method for finding differentially expressed genes in single-cell transcriptome data. Nature Communications, 2020, 11, 4318.	5.8	50
7	Codon bias confers stability to human <scp>mRNA</scp> s. EMBO Reports, 2019, 20, e48220.	2.0	100
8	Pulmonary Regnase-1 orchestrates the interplay of epithelium and adaptive immune systems to protect against pneumonia. Mucosal Immunology, 2018, 11, 1203-1218.	2.7	23
9	Waves of chromatin modifications in mouse dendritic cells in response to LPS stimulation. Genome Biology, 2018, 19, 138.	3.8	19
10	Microarray analysis of macrophage response to infection with Streptococcus oralis reveals the immunosuppressive effect of hydrogen peroxide. Biochemical and Biophysical Research Communications, 2017, 485, 461-467.	1.0	8
11	Microarray and gene co-expression analysis reveals that melatonin attenuates immune responses and modulates actin rearrangement in macrophages. Biochemical and Biophysical Research Communications, 2017, 485, 414-420.	1.0	18
12	Regnase-1 Maintains Iron Homeostasis via the Degradation of Transferrin Receptor 1 and Prolyl-Hydroxylase-Domain-Containing Protein 3 mRNAs. Cell Reports, 2017, 19, 1614-1630.	2.9	54
13	Guidance of regulatory T cell development by Satb1-dependent super-enhancer establishment. Nature Immunology, 2017, 18, 173-183.	7.0	300
14	Mapping circulating serum miRNAs to their immune-related target mRNAs. Advances and Applications in Bioinformatics and Chemistry, 2017, Volume 10, 1-9.	1.6	4
15	Modeling the <i>cis</i> -regulatory modules of genes expressed in developmental stages of <i>Drosophila melanogaster</i> . PeerJ, 2017, 5, e3389.	0.9	2
16	A rare subset of skin-tropic regulatory T cells expressing Il10/Gzmb inhibits the cutaneous immune response. Scientific Reports, 2016, 6, 35002.	1.6	36
17	Genome-wide map of RNA degradation kinetics patterns in dendritic cells after LPS stimulation facilitates identification of primary sequence and secondary structure motifs in mRNAs. BMC Genomics, 2016, 17, 1032.	1.2	15
18	Immuno-Navigator, a batch-corrected coexpression database, reveals cell type-specific gene networks in the immune system. Proceedings of the National Academy of Sciences of the United States of America, 2016, 113, E2393-402.	3.3	58

ALEXIS VANDENBON

#	Article	IF	CITATIONS
19	Regnase-1 and Roquin Regulate a Common Element in Inflammatory mRNAs by Spatiotemporally Distinct Mechanisms. Cell, 2015, 161, 1058-1073.	13.5	296
20	Hydroxypropyl-β-Cyclodextrin Spikes Local Inflammation That Induces Th2 Cell and T Follicular Helper Cell Responses to the Coadministered Antigen. Journal of Immunology, 2015, 194, 2673-2682.	0.4	64
21	A Set of Structural Features Defines the Cis-Regulatory Modules of Antenna-Expressed Genes in Drosophila melanogaster. PLoS ONE, 2014, 9, e104342.	1.1	2
22	Differential roles of epigenetic changes and Foxp3 expression in regulatory T cell-specific transcriptional regulation. Proceedings of the National Academy of Sciences of the United States of America, 2014, 111, 5289-5294.	3.3	111
23	Akirin2 is critical for inducing inflammatory genes by bridging lκBâ€Î¶ and the <scp>SWI</scp> / <scp>SNF</scp> complex. EMBO Journal, 2014, 33, 2332-2348.	3.5	105
24	Dynamics of enhancers in myeloid antigen presenting cells upon LPS stimulation. BMC Genomics, 2014, 15, S4.	1.2	2
25	A Parzen window-based approach for the detection of locally enriched transcription factor binding sites. BMC Bioinformatics, 2013, 14, 26.	1.2	4
26	Malt1-Induced Cleavage of Regnase-1 in CD4+ Helper T Cells Regulates Immune Activation. Cell, 2013, 153, 1036-1049.	13.5	296
27	The Transcription Factor Jdp2 Controls Bone Homeostasis and Antibacterial Immunity by Regulating Osteoclast and Neutrophil Differentiation. Immunity, 2012, 37, 1024-1036.	6.6	70
28	A novel unbiased measure for motif co-occurrence predicts combinatorial regulation of transcription. BMC Genomics, 2012, 13, S11.	1.2	12
29	Systems biology approaches to tollâ€like receptor signaling. Wiley Interdisciplinary Reviews: Systems Biology and Medicine, 2012, 4, 497-507.	6.6	17
30	Stochastic binary modeling of cells in continuous time as an alternative to biochemical reaction equations. Physical Review E, 2011, 84, 062903.	0.8	4
31	The Jmjd3-Irf4 axis regulates M2 macrophage polarization and host responses against helminth infection. Nature Immunology, 2010, 11, 936-944.	7.0	996
32	Modeling tissue-specific structural patterns in human and mouse promoters. Nucleic Acids Research, 2010, 38, 17-25.	6.5	73
33	lκBζ is essential for natural killer cell activation in response to IL-12 and IL-18. Proceedings of the National Academy of Sciences of the United States of America, 2010, 107, 17680-17685.	3.3	46
34	Markov Chain-based Promoter Structure Modeling for Tissue-specific Expression Pattern Prediction. DNA Research, 2008, 15, 3-11.	1.5	7
35	USING SIMPLE RULES ON PRESENCE AND POSITIONING OF MOTIFS FOR PROMOTER STRUCTURE MODELING AND TISSUE-SPECIFIC EXPRESSION PREDICTION. , 2008, , .		1
36	Using simple rules on presence and positioning of motifs for promoter structure modeling and tissue-specific expression prediction. Genome Informatics, 2008, 21, 188-99.	0.4	2